J. Fluid Mech. (1972), *vol.* 52, *part* 2, *pp.* 357–367
Printed in Great Britain

Boundary-layer velocity profiles in a swirling convergent flow field

By T. M. HOULIHAN AND D. J. HORNSTRA
Mechanical Engineering Department, Naval Postgraduate School, Monterey, California

(Received 28 December 1970 and in revised form 10 November 1971)

Velocity distributions within the boundary layer of a swirling flow of incompressible fluid in a convergent conical nozzle have been investigated. Theoretical calculations with boundary conditions more appropriate to physically existent situations discounted the existence of 'super-velocities' within the boundary layer. Parallel experimental investigations demonstrated an interdependence of core and boundary-layer flows which precluded the maintenance of the flow conditions required by the analysis.

1. Introduction

Velocity profiles in the laminar boundary layer of a swirling convergent flow field were first investigated by Taylor (1950). He considered the case of a dominant tangential flow superimposed upon a secondary axial flow in a conical nozzle. Applying the Pohlhausen method to the momentum integral equations of the problem, Taylor concluded that operating conditions could arise whereby most of the nozzle discharge was caused by the flow within the boundary layer at the wall of the swirl chamber. Binnie & Harris (1950) extended Taylor's approach to include radial as well as swirling flow in a conical Venturi geometry.

Wilks (1968) re-examined the laminar boundary layer in a swirling nozzle flow. He considered the flow field to be composed of a central inviscid core flow plus a thin boundary-layer flow at the walls of the swirl chamber. The inviscid core contained two flow components: a uniform axial flow and a free vortex flow aligned concentrically with the centre-line of the nozzle. Using Weighardt's two-parameter integral technique, Wilks demonstrated the possibility of 'super-velocities', i.e. velocities greater than free-stream velocities, existing within the boundary layer.

In this paper, an approach analogous to that of Wilks was used. Here, however, the effect of boundary-layer growth upon the tangential and axial velocities in the free-stream flow was taken into consideration. As a result, no 'super-velocities' were found to exist within the boundary layer of the swirling conical nozzle flow investigated. Furthermore, experimental results proved that rotational effects (not boundary-layer effects) were of paramount importance in the convergent swirling flow configuration tested.

2. Previous theory

Following Wilks, a curvilinear co-ordinate system is defined with the x axis along the wall and the z axis perpendicular to the wall of the nozzle. The shape of the nozzle is determined by the surface of revolution of an arbitrary curve $r(x)$ (see figure 1).

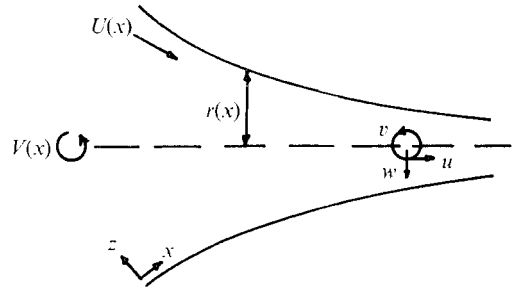

FIGURE 1. Co-ordinate system.

The momentum integral equations of the problem are

$$\left.\begin{aligned} \frac{1}{r}\frac{d}{dx}\left(r\int_0^\infty u(u-U)\,dz\right)+\frac{dU}{dx}\int_0^\infty (u-U)\,dz+\frac{r'}{r}\int_0^\infty (V^2-v^2)\,dz &= -\nu\left(\frac{\partial v}{\partial z}\right)_0, \\ \frac{1}{r^2}\frac{d}{dx}\left(r^2\int_0^\infty u(v-V)\,dz\right) &= -\nu\left(\frac{\partial v}{\partial z}\right)_0, \end{aligned}\right\} \tag{1}$$

with boundary conditions

$$\left.\begin{aligned} &u=0, \quad -\nu\frac{\partial^2 u}{\partial z^2}=U\frac{dU}{dx}-V^2\frac{r'}{r} \quad \text{on} \quad z=0, \\ &u=U(x), \quad \frac{\partial u}{\partial z}=0, \quad \frac{\partial^2 u}{\partial z^2}=0 \quad \text{when} \quad z\to\infty, \\ &v=0 \quad \frac{\partial^2 v}{\partial z^2}=0 \quad \text{on} \quad z=0, \\ &v=V(x)=\frac{A}{r(x)}, \quad \frac{\partial v}{\partial z}=0, \quad \frac{\partial^2 v}{\partial z^2}=0 \quad \text{when} \quad z\to\infty. \end{aligned}\right\} \tag{2}$$

Distances in the above equations are normalized by defining $n = z/\delta$ and $s = x/c$, where δ is the local boundary-layer thickness and c is the distance along the generator of the nozzle to its apex.

To obtain a solution of the integral momentum equations, the two-parameter method of Weighardt involving an eleventh-degree polynomial is used. Applying both parameters to the axial profile in the boundary layer (assuming that the tangential profile is not altered significantly with downstream distance s) yields

$$u/U = f_1(n)+L_1 f_2(n)+L_2 f_3(n),$$

where

$$\left.\begin{aligned} f_1(n) &= 1-(1-n)^8(1+8n+36n^2+120n), \\ f_2(n) &= 1-n)^8 n(1+8n+36n^2), \\ f_3(n) &= -(1-n)^8 n^2(1+8n). \end{aligned}\right\} \tag{3}$$

From the boundary conditions, the polynomial corresponding to the swirl profile is

$$v/V = g(n) = 2n - 2n^3 + n^4. \tag{4}$$

Evaluation of the axial velocity profile at the wall leads to physical connotations for the shape factors L_1 and L_2. L_1 involves wall shear stress, whereas L_2 reflects axial pressure gradient behaviour:

$$L_1 = \frac{\tau\delta}{\mu U}, \quad L_2 = \frac{\delta}{2c}\frac{\delta}{\mu U}\left(-\frac{dP}{dx}\right). \tag{5}$$

Following Wilks, coefficients A_1, A_2, A_3 and A_4 (ratios of characteristic thicknesses) are defined (see appendix A) and the term

$$G = (U\delta/\nu)(\delta/c) \tag{6}$$

is introduced, giving

$$\left.\begin{aligned} \frac{r'}{r} + \frac{U'}{U}(2 + A_1) + \frac{\delta'_{2x}}{\delta_{2x}} &= \frac{A_2}{G} + \frac{r'}{r}\left(\frac{V}{U}\right)^2 A_3, \\ \frac{r'}{r} + \frac{U'}{U} + \frac{\delta'_{2xy}}{\delta_{2xy}} &= \frac{A_4}{G}. \end{aligned}\right\} \tag{7}$$

As a method of simplifying the solution, a basically linear relationship is assumed to exist between the momentum thickness δ_{2x} and the boundary-layer thickness δ and between the mixed momentum thickness δ_{2xy} and the boundary-layer thickness. The above equations are then combined with the definitions of G and its derivative to give the following relationships:

$$G' = 2A_4 - \frac{(A_2 - A_4)}{(A_1 - 1)} - G\frac{r'}{r}\left[2 + \left(\frac{V}{U}\right)^2 \frac{A_3}{(1 + A_1)}\right], \tag{8}$$

$$A_2 = G\frac{U'}{U}(1 + A_1) + A_4 - G\frac{r'}{r}\left(\frac{V}{U}\right)^2 A_3, \tag{9}$$

$$L_2 = \frac{G}{2}\left[\frac{U'}{U} - \left(\frac{V}{U}\right)^2 \frac{r'}{r}\right]. \tag{10}$$

Finally an iterative procedure is used to solve the governing equations for various values of downstream distance s.

Hornstra (1970) developed a modification of this theory to accommodate an initial non-zero boundary-layer thickness. He then solved the resulting equations for various values of the swirl factor ($K = V_0/U_0$) and initial boundary-layer thickness. The results shown in figures 2 and 3 indicate that the 'super-velocity' values produced by these formulations increase dramatically as both the swirl factor and downstream distance increase.

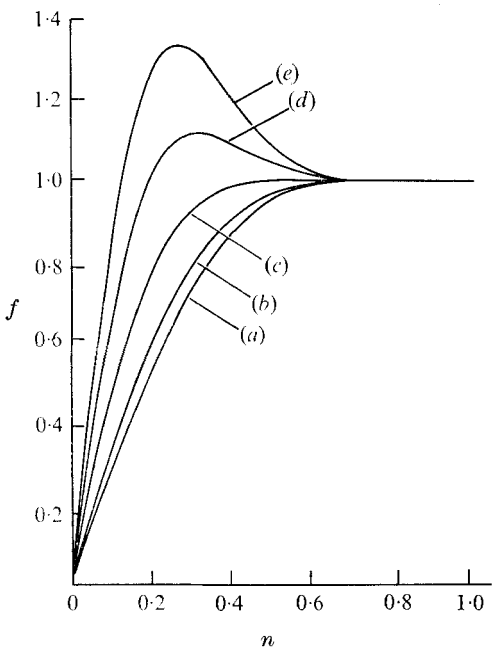

FIGURE 2. Variations in profile with K. $X = 0{\cdot}1$, $G(0) = 0$. (*a*) $K = 0$, (*b*) $K = 1$, (*c*) $K = 2$, (*d*) $K = 3$, (*e*) $K = 4$.

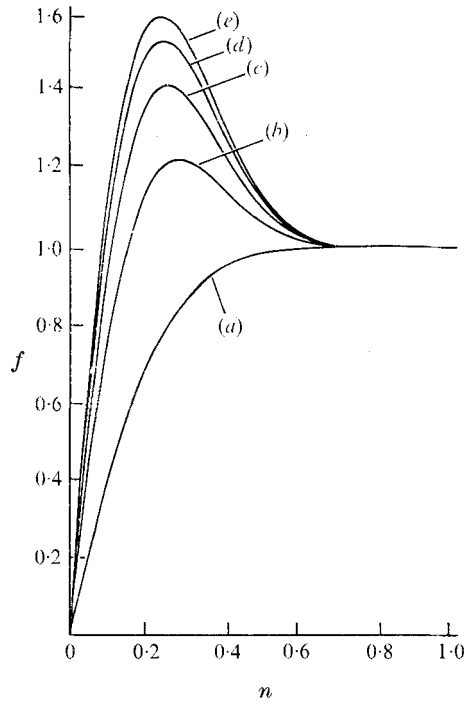

FIGURE 3. Variations in profile with x. $K = 4$, $G(0) = 0{\cdot}52$ (*a*) $x = 0$, (*b*) $x = 0{\cdot}05$, (*c*) $x = 0{\cdot}10$, (*d*) $x = 0{\cdot}15$, (*e*) $x = 0{\cdot}20$.

3. Present theory

Wilks assumed that the tangential velocity at the outer edge of the boundary layer could be described as $V = A/r$, where A is a swirl constant. This assumption is only appropriate if the boundary-layer thickness is small compared to the value of r. Yet Wilks's numerical solution led to a boundary-layer growth of the same order of magnitude as the radius for air flow in a conical nozzle of inlet radius of 1 in. with an initial axial velocity of 1 ft/s.

For a boundary-layer growth of such magnitude, it is to be observed that tangential velocity would reach free-stream value at the boundary-layer–core-flow interface. Thus, to describe the behaviour of this convergent swirling flow field correctly, the tangential flow distribution must realize this consequence of boundary-layer growth. A free-stream tangential velocity profile which would adequately account for this extensive boundary-layer growth would be one of the form $V = A/(r-\delta)$. In contrast, Wilks's formulation, viz. $V = A/r$, implies that the tangential velocity reaches the free-stream value at the wall, rather than at the interface.

With this in mind, King (1967) produced the first solutions which describe the full behaviour of the core in a swirling convergent nozzle flow by likewise changing the basis of application of the boundary conditions on tangential flow

from the wall of the swirl chamber to the core-flow–boundary-layer interface. Introducing the modified value of V, $V = A/(r-\delta)$, altered the tangential momentum integral equation. By incorporating the definition of a new thickness

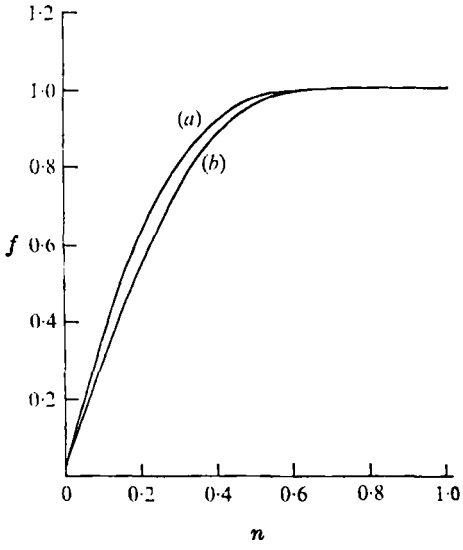

FIGURE 4. Comparison of theoretical curves. $K = 1$, $x = 0{\cdot}1$, $G(0) = 0{\cdot}52$, $\delta(0)/r_0 = 0{\cdot}130$. (*a*) Wilks theory. (*b*) Present theory.

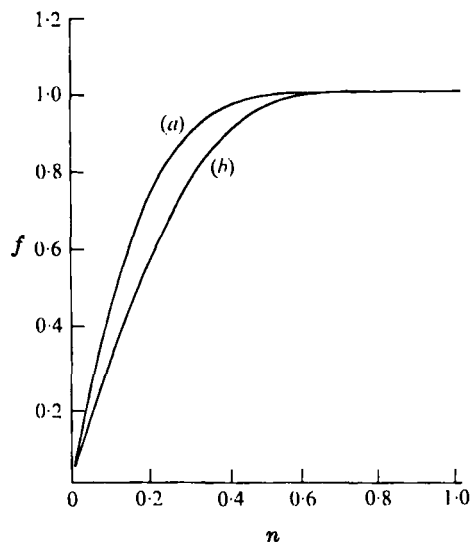

FIGURE 5. Comparison of theoretical curves. $K = 1$, $x = 0{\cdot}2$, $G(0) = 0{\cdot}52$, $\delta(0)/r_0 = 0{\cdot}130$. (*a*) Wilks theory. (*b*) Present theory.

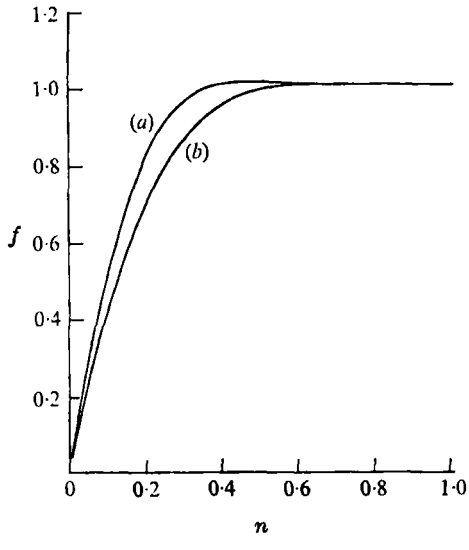

FIGURE 6. Comparison of theoretical curves. $K = 2$, $x = 0{\cdot}1$, $G(0) = 0{\cdot}52$, $\delta(0)/r_0 = 0{\cdot}130$. (*a*) Wilks theory. (*b*) Present theory.

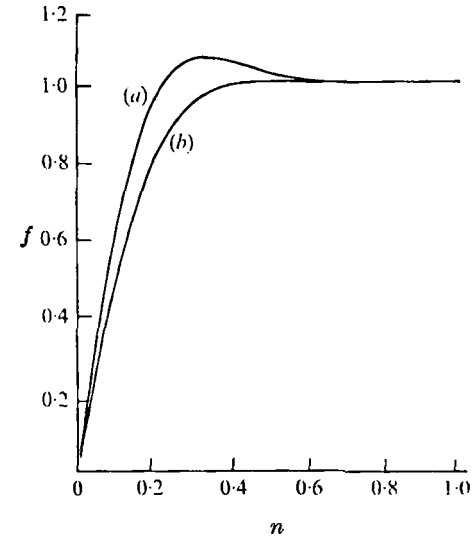

FIGURE 7. Comparison of theoretical curves. $K = 2$, $x = 0{\cdot}2$, $G(0) = 0{\cdot}152$ $\delta(0)/r_0 = 0{\cdot}130$. (*a*) Wilks theory. (*b*) Present theory.

coefficient A_5 (appendix B), the modified momentum integral equation for the tangential flow thus became

$$\frac{r'}{r}+\frac{U'}{U}+\frac{\delta'}{\delta}+\left[\frac{r'}{r}+\frac{V'}{V}+\left(\frac{A_5}{(r/\delta)-1}\right)\left(\frac{\delta'}{\delta}-\frac{r'}{r}\right)\right]=\frac{A_4}{G}. \tag{11}$$

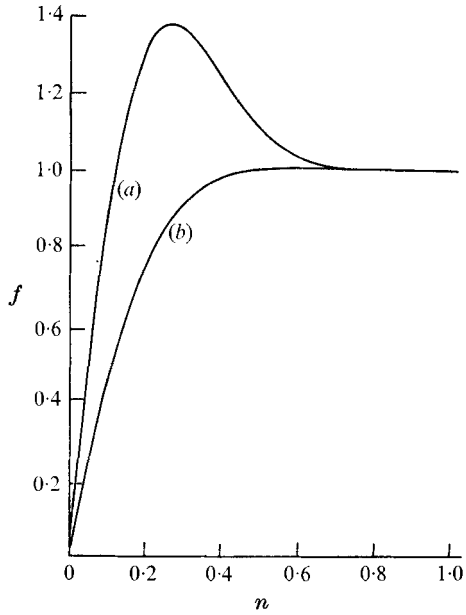

FIGURE 8. Comparison of theoretical curves. $K = 4$, $x = 0{\cdot}1$, $G(0) = 0{\cdot}26$, $\delta(0)/r_0 = 0{\cdot}065$. (*a*) Wilks theory. (*b*) Present theory.

Here, the assumption of a basically linear relationship between characteristic thicknesses was used. The terms in the square brackets represent the terms added to Wilks's original tangential-flow momentum integral equation by the new assumption, i.e. $V = A/(r-\delta)$. Also, if the boundary layer is thick enough to affect the tangential flow it is reasonable to assume that axial flow would likewise be affected by the increased boundary-layer thickness. This added consequence of boundary-layer growth was accounted for in this analysis by using the value of radius minus displacement thickness, rather than radius alone, in the axial-flow continuity equation (see appendix B). This alteration of the free-stream axial-flow velocity value did not affect the derivation of the axial momentum equation. However, final computations involving the axial momentum equation necessitated the calculation of the axial velocity and its derivative. Hence the value of the displacement thickness and its derivative were required. Boundary-layer thickness at any point was easily calculated from the value of the function G. The calculation of the derivative of displacement thickness was not so direct.

However, since a basically linear relationship was presumed to exist between displacement thickness and boundary-layer thickness, the ratio of the displacement thickness to its derivative was recognized as being equal to the ratio of the

boundary-layer thickness to its derivative. With these determinations and with equation (11) as the swirl momentum integral, the momentum integral equations were solved for various normalized values of the initial boundary-layer thickness, the initial velocity and the swirl factor. Results are shown in figures 4–8. The solutions showed no sign of the existence of super-velocity components.

4. Experimentation

An apparatus (figure 9) analogous to that used by Lay (1950) was constructed to test the velocity distribution assumed by the theory, viz. a combination of a free line vortex and uniform axial flow. To ensure laminar pipe flow of air at speeds of at least 2 ft/s a pipe diameter of 2 in. was chosen. The shape of the axial flow

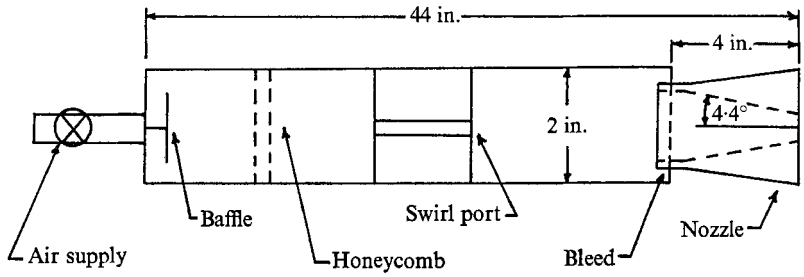

FIGURE 9. Schematic diagram of experimental apparatus.

entering the swirl chamber was varied by adjusting the axial position of the annular honeycomb flow straightener. Air was introduced tangentially into the axial flow through a port in the wall of the pipe. The area of the port was variable, thus providing fine adjustment of the swirl factor.

Lay's tests indicated that close to the wall there is a region where tangential flow is retarded by viscosity. This region interacts with the boundary layer of the axial flow and thus augments the boundary-layer region. To avoid this enhanced boundary-layer growth, the outer annular portion of the flow was bled to the atmosphere and thus only a 'flat' inner portion of the swirling flow entered the conical nozzle. The position of the 0·77 in. radius nozzle, relative to the end of the surrounding 1 in. pipe, could be altered in order to vary the amount of flow bled off. The nozzle itself (semi-angle 4.4°) contained a straight inlet section, 1 in. in length, which ensured the continuation of proper flow characteristics following bleed-off. The distance along the generator of the cone to the apex (called c in the analysis) was 10 in. The truncated cone used in the test apparatus extended over $0{\cdot}35\,c$. All flow conditions, both axial and tangential, were monitored with two linearized Disa 55D01 hot-wire anemometers.

In all cases tested (see figures 10 (a)–(d)) the velocity distribution in the core flow changed drastically with downstream distance. Thus, the initial combination of a 'flat' axial profile and a free vortex which extended over a major portion of the inlet cross-section was destroyed immediately downstream of the inlet.

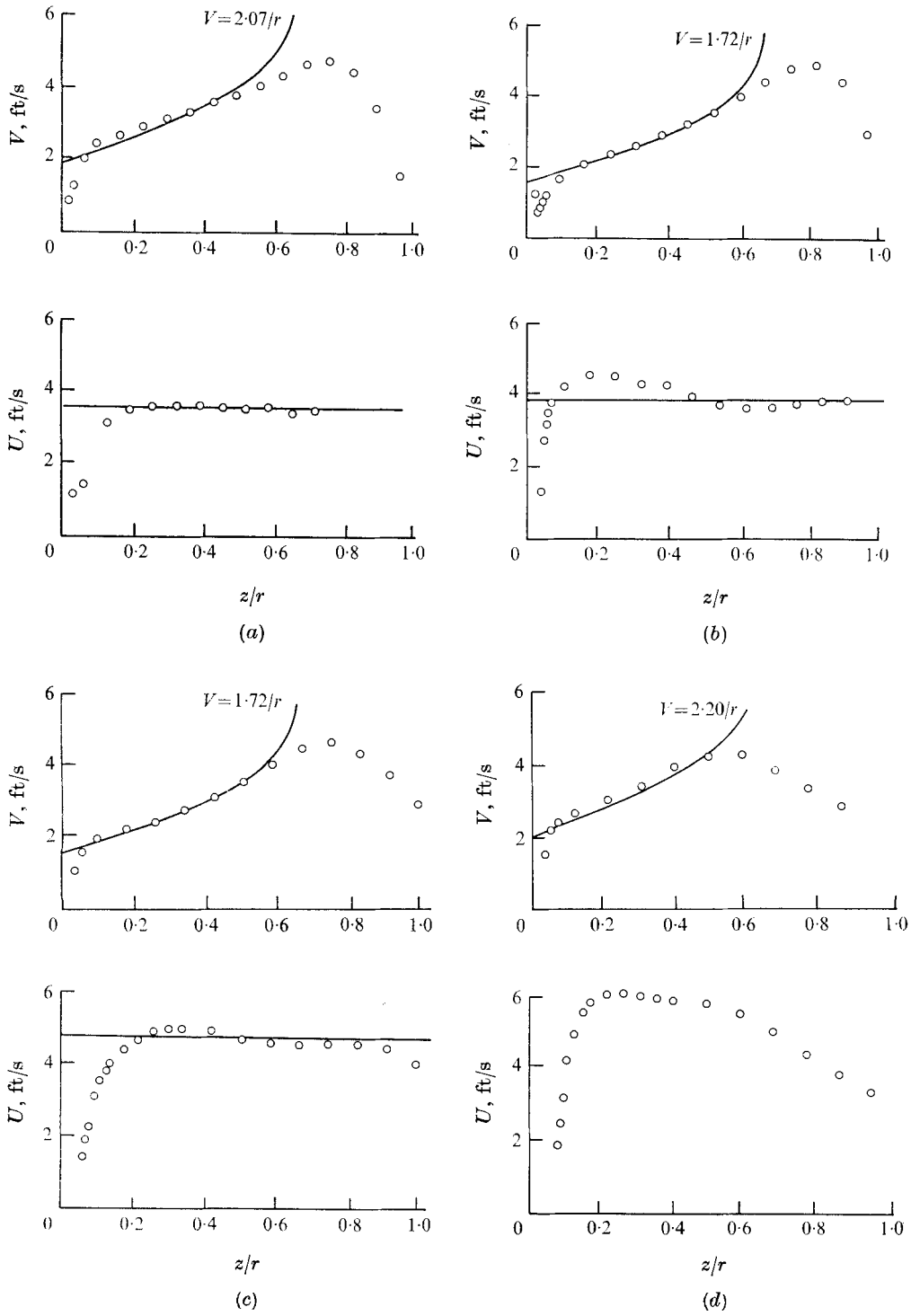

FIGURE 10. Experimental velocity profiles. $K = 0{\cdot}8$, (*a*) $x = 0$, (*b*) $x = 0{\cdot}1$, (*c*) $x = 0{\cdot}2$, (*d*) $x = 0{\cdot}3$.

Hence a close experimental check of the theory was impossible to perform. Generally, low values of swirl resulted in an axial flow that resembled pipe flow in distribution, whereas high values of swirl caused formation of a vortex flow which featured high axial velocities at the core extremities. However, at no time were any 'super-velocities' recorded as occurring within the boundary layer of the swirl chamber.

5. Conclusions

In considering the swirling flow within the boundary layer of a convergent nozzle, Wilks assumed a flow configuration comprised of a core flow consisting of a free vortex, combined with a uniform axial flow enveloped by a thin boundary layer. Thus core velocities were dependent only upon the geometric configuration of the convergent nozzle. A further assumption, viz. that a linear relationship existed between the various characteristic thicknesses of the problem, led to a solution of the momentum integral equations which featured the appearance of a super-velocity within the boundary layer of the swirl chamber. In the present analysis, for low velocity air flow (required to maintain laminar flow conditions) it was shown theoretically that the assumed boundary-layer growth in the swirl chamber was definitely not negligible, being of the order of the radius of the swirl chamber under some operating conditions. Thus, incorporating this growth into the boundary values of the problem, i.e. by changing the base of application of these boundary values, as did King (1967) in a related problem, solutions corresponding to the altered momentum integral equations were found to exhibit no super-velocity phenomena.

Furthermore, parallel experiments have demonstrated that, even when one attains the initial flow conditions necessitated by the analysis, these conditions are subsequently altered in a short distance downstream by the boundary-layer–core-flow interplay. Thus, since the major portion of the flow field is changing so rapidly in this manner, it does not seem worthwhile to concentrate upon a minor portion of the flow field, viz. the boundary layer, in order to analyse the characteristics of the flow occurring throughout this swirling domain.

Finally, in all the theories presented so far, it was assumed that a basically linear relationship exists between the various characteristic thicknesses of the flow. Since these thicknesses are functions of the shape factors, which are in turn functions of downstream distance [i.e. $L_1(\delta)$ and $L_2(\delta)$], it would seem mandatory to extend these analyses without the restrictive assumption of the existence of a linear relationship.

Appendix A. Previous theory

From Wilks (1968)

$$A_1 = \frac{\int_0^1 (1-f)\,dn}{\int_0^1 f(1-f)\,dn} = \frac{\delta_{1x}}{\delta_{2x}} = \frac{D_1}{D_2}, \quad A_2 = \frac{f'(0)}{\int_0^1 f(1-f)\,dn} = \frac{L_1}{D_2},$$

$$A_3 = \frac{\int_0^1 (1-g^2)\,dn}{\int_0^1 f(1-f)\,dn} = \frac{D_4}{D_2}, \qquad A_4 = \frac{g''(0)}{\int_0^1 (f(1-g)\,dn} = \frac{2}{D_3}.$$

Integration of the polynomial expressions for the velocity ratios (f and g) in the above integrals yields

$$D_1 = 0{\cdot}3333 - 0{\cdot}0454L_1 + 0{\cdot}0061L_2,$$
$$D_2 = 0{\cdot}0740 - 0{\cdot}0149L_1 - 0{\cdot}0012L_2 - 0{\cdot}0045L_1^2 - 0{\cdot}00008L_2^2 + 0{\cdot}0012L_1L_2,$$
$$D_3 = 0{\cdot}0846 + 0{\cdot}0244L_1 - 0{\cdot}0029L_2, \quad D_4 = 0{\cdot}4175.$$

For a conic nozzle $r(s) = r_0(1-s)$, and from continuity

$$\pi r_0^2 U_0 = \pi r^2 U,$$
$$U(s) = U_0/(1-s)^2,$$
$$V(s) = KU_0/(1-s).$$

Conservation of angular momentum requires that $r_0 V_0 = rV = A$. If

$$V_0 = KU_0, \quad \text{then} \quad V(s) = KU_0/(1-s).$$

Appendix B. Present theory

With $V = A/(r-\delta)$ as $z \to \infty$, the V momentum equation is altered as follows:

$$V\left(\frac{\partial u}{\partial x}\right) = \frac{\partial (uV)}{\partial x} - u\left(\frac{\partial V}{\partial x}\right) = \frac{\partial (uV)}{\partial x} + \frac{uV}{r-\delta}\left(\frac{dr}{dx} - \frac{d\delta}{dx}\right),$$

$$\int_0^\infty \left[\frac{\partial}{\partial x}(uv - Vu) + \frac{2u}{r}(u-V)\frac{dr}{dx} + \frac{uV}{r}\frac{dr}{dx} + \frac{uV}{r-\delta}\left(\frac{d\delta}{dx} - \frac{dr}{dx}\right)\right] dz = -\nu\left(\frac{\partial v}{\partial z}\right)_0.$$

Simplifying,

$$\frac{1}{r^2}\frac{d}{dx}\left(r^2 \int_0^\infty u(v-V)\,dz\right) + \frac{V}{r-\delta}\left(\frac{d\delta}{dx} - \frac{\delta}{r}\frac{dr}{dx}\right)\int_0^\infty u\,dz = -\nu\left(\frac{\partial v}{\partial z}\right)_0.$$

Introducing the two-parameter velocity profiles into this expression gives

$$\frac{1}{r^2 c}\frac{d}{ds}\left(r^2 U V \delta \int_0^1 f(1-g)\,dn\right) + \frac{uV}{r-\delta}\frac{1}{c}\left(\frac{d\delta}{ds} - \frac{\delta}{r}\frac{dr}{ds}\right)\delta \int_0^1 f\,dn = -\left(\nu\frac{A}{\delta r}\right)g'(0),$$

with boundary conditions

$$g = 0, \quad g'' = 0, \qquad\qquad \text{on} \quad n = 0,$$
$$g = 1, \quad g' = 0, \quad g'' = 0, \quad \text{on} \quad n = 1.$$

The corresponding axial momentum equation is

$$\frac{1}{rc}\frac{d}{ds}\left(rU^2\delta\int_0^1 f(f-1)\,dn\right)+\frac{dU}{ds}\frac{U\delta}{c}\int_0^1(f-1)\,dn+\frac{1}{cr}V^2\frac{dr}{ds}\delta\int_0^1(1-g^2)\,dn = -\nu\frac{U}{\delta}f'(0),$$

with boundary conditions

$$f=0,\left(\frac{-\nu U}{\delta^2}\right)f''=\frac{U}{c}\frac{dU}{ds}-\frac{V^2}{rc}\frac{dr}{ds}\quad\text{at}\quad n=0,$$

$$f=1,\quad f'=0,\quad f''=0\quad\text{at}\quad n=1.$$

Defining coefficients A_1, A_2, A_3 and A_4 as in appendix A, introducing a new term

$$\int_0^1 f\,dn\Big/\int_0^1 f(1-g)\,dn=(1-D_1)/D_3$$

and assuming that a nominally linear relationship exists between the characteristic thicknesses of the problem yields the final forms of the momentum integral equations for the problem:

$$\frac{r'}{r}+\frac{U'}{U}(2+A_1)+\frac{\delta'}{\delta}=\frac{A_2}{G}+\frac{r'}{r}\left(\frac{V}{U}\right)^2A_3\frac{2r'}{r}+\frac{U'}{U}+\frac{V'}{V}+\frac{\delta'}{\delta}+\frac{1}{(r/\delta)-1}\left(\frac{\delta'}{\delta}-\frac{r'}{r}\right)A_5=\frac{A_4}{G}.$$

Taking displacement thickness into consideration, the continuity equation for axial flow becomes

$$\pi(r_0-\delta_{1x}(0))^2U_0=\pi(r_0(1-s)-\delta_{1x}(s))^2U(s),$$

$$U(s)=U_0\frac{[1-(\delta_{1x}(0)/r_0)]^2}{[(1-s)-(\delta_{1x}(s)/r_0)]^2}.$$

Further,

$$\frac{U'}{U}=\frac{2(1+\delta'_{1x}(s)/r_0)}{[(1-s)-(\delta_{1x}(s)/r_0)]}.$$

With $V=A/(r-s)$, conservation of angular momentum yields

$$[r_0-\delta(0)]\,V_0=[r_0(1-s)-\delta(s)]\,V(s),$$

$$V(s)=\frac{KU_0[1-(\delta(0)/r_0)]}{[(1-s)-(\delta(s)/r_0)]}.$$

REFERENCES

Binnie, A. M. & Harris, D. P. 1950 *Quart. J. Mech. Appl. Math.* **3**, 89.

Hornstra, D. J. 1970 MSc. Thesis, Naval Postgraduate School, Monterey, California.

King, W. S. 1967 Ph.D. dissertation, University of California, Los Angeles.

Lay, J. E. 1950 *J. Heat Transfer*, **1**, 205.

Taylor, G. I. 1950 *Quart. J. Mech. Appl. Math.* **3**, 129.

Wilks, G. 1968 *J. Fluid Mech.* **34**, 575.